Dynamical properties of strongly coupled electronic bilayers: A molecular dynamics study

R. E. Johnson
Department of Mathematics and Computer Science, Royal Military College of Canada, Kingston, Ontario, Canada K7K 7B4

S. Ranganathan
Department of Physics, Royal Military College of Canada, Kingston, Ontario, Canada K7K 7B4

(Received 28 July 2003; published 19 February 2004)

Extensive molecular dynamics (MD) calculations have been performed for a classical symmetric electronic bilayer system for various values of the coupling parameter Γ and interlayer separation d. Static structure factors were obtained, but the emphasis was on dynamic correlation functions, in particular the intralayer and interlayer intermediate scattering functions $F(q,t)$ and their Fourier transforms $S(q,\omega)$. Results and analysis are presented here mainly for the plasma parameter $\Gamma=80$, where previous MD studies have shown dramatic changes in certain properties of the system for intermediate values of d. Significant variations in the dynamic structure factors $S(q,\omega)$ with interlayer separation are observed and a detailed discussion is presented. An emergence of two side peaks is noted for certain values of wave vector q and interlayer separation d; this novel behavior appears only for high values of Γ.

DOI: 10.1103/PhysRevB.69.085309 PACS number(s): 73.21.Ac, 73.22.Lp, 61.20.Ja

I. INTRODUCTION

Strongly coupled electronic bilayers have been the focus of research in recent years. A classical bilayer consists of two parallel plane layers of charged particles obeying classical statistical mechanics. It can be characterized by two parameters: the interlayer separation distance d and the coupling parameter $\Gamma=e^2/(ak_BT)$, where $a=(n\pi)^{-1/2}$ is the Wigner-Seitz radius, e the electronic charge, and n the surface density of particles. Zero temperature ($\Gamma=\infty$) lattice dynamics calculations of a classical bilayer predict a sequence of five structural phase changes, with increasing d.[1] Such a sequence has been observed in Monte Carlo (MC) simulations in the solid phase ($\Gamma=165$) of a bilayer.[2] Note that a classical single layer, two-dimensional electron gas (2DEG) has been shown to exhibit a fluid-solid transition between $\Gamma=120$ and 130. Molecular dynamics (MD) simulations have revealed the presence of structural phases at intermediate d, even when the system is in a fluid state for large d. For example, MD calculations for $\Gamma=80$ and d near $0.8a$ have shown the appearance of a pronounced long-range order in the intralayer and interlayer pair correlation functions,[3,4] and a large reduction in the diffusion coefficient.[4] For this value of d the bilayer exhibits a staggered-square structural phase, and MC simulations have found the highest melting temperature.[5] MD analyses of single particle properties such as the velocity correlation function and self-intermediate scattering function corroborate the existence of solidlike structures in such strongly coupled bilayers.[6]

There have been some theoretical studies of the dynamical properties of strongly coupled bilayers.[7–10] However, a lack of sufficient and detailed experimental and MD data has impeded progress in the understanding of these systems. Limited experimental data is available,[11–13] but since experiments involve complex and quantum systems, their results are not immediately applicable to classical bilayer systems. One then has to depend on MD generated results with which to compare the predictions of any theoretical model. In this paper, we provide some of the needed MD data for certain dynamical correlation functions of a strongly coupled, classical bilayer.

II. SIMULATION DETAILS

The system to be simulated is a bilayer consisting of classical electrons interacting through the $1/r$ Coulomb potential. The single-component bilayer is equivalent to a two-component single-layer system with an interaction potential matrix $V_{11}(r)=V_{22}(r)=e^2/r$ and $V_{12}(r)=V_{21}(r)=e^2/\sqrt{r^2+d^2}$. The system is identical to the one used by us previously to investigate diffusion and single-particle properties, but we describe it here for completeness. The electrons are distributed evenly in two planes separated by a constant distance and are not allowed to move out of the planes. Charge neutrality is guaranteed by embedding the electrons in a uniform background of opposite charge. In each layer the basic simulation cell is a square and periodic boundary conditions are imposed. The number of electrons per cell in each of the layers was chosen to be 512. A larger number of particles increases the statistics considerably, and hence decreases the errors of the dynamical correlation functions which we obtain. It also allows the use of more and smaller values of the wave vector q that can be used in the evaluation of the correlation functions.

A thermodynamic state of the system is entirely specified by the dimensionless plasma coupling parameter Γ and the interlayer separation d which, in what follows, is expressed in units of a. Only symmetric bilayers, in which the density of the electrons is the same in both layers, are considered in this study. All quantities involved are in dimensionless units: distance in units of WS radius a, wave vector q in units of $1/a$, time in units of $\tau=\sqrt{ma^3/e^2}$, where m is the electron mass and frequency ω in units of $1/\tau$. The two layers have the same surface density and the basic cell is a square with side length $L=(N/na^2)^{1/2}$, containing $N=512$ electrons in each of the two layers. Since a is the unit of length, the density in each layer takes the value $1/\pi$; this gives L

$=40.1$ in dimensionless units. The details of the simulation and of the extended Ewald sum technique used in our dynamics algorithm have been described in our previous papers.[4,14]

After the equilibrium configuration has been achieved, the two-dimensional position and velocity components of each of the electrons in the two planes were computed for 20 000 time steps, with the step length chosen to be 0.03. These were stored for $t_j=0.6j$ with j from 1 to $M=10\,000$. The position coordinates at time t_j are labeled by $\vec{r}_k(t_j)=\{x_k(t_j),y_k(t_j)\}$ where $k=1$ to N for layer 1 and $k=N+1$ to $2N$ for layer 2. These components were then used to calculate the correlation functions of interest.

The collective properties of the system are contained in the dynamical correlation functions: the intermediate scattering functions $F_{11}(q,t)$ and $F_{12}(q,t)$, and their respective Fourier transforms $S_{11}(q,\omega)$ and $S_{12}(q,\omega)$, the dynamic structure factors. They are defined as

$$F_{11}(q,t)=\langle\rho_1(\vec{q},t)\rho_1(-\vec{q},0)\rangle,$$

$$F_{12}(q,t)=\langle\rho_1(\vec{q},t)\rho_2(-\vec{q},0)\rangle, \tag{1}$$

where

$$\rho_1(\vec{q},t)=\frac{1}{\sqrt{N}}\sum_{k=1}^{N}\exp[i\vec{q}\circ\vec{r}_k(t)],$$

$$\rho_2(\vec{q},t)=\frac{1}{\sqrt{N}}\sum_{k=N+1}^{2N}\exp[i\vec{q}\circ\vec{r}_k(t)] \tag{2}$$

are the density fluctuations. Because of symmetry, the roles of the two layers can be interchanged. The dynamic structure factors are defined as

$$S_{11}(q,\omega)=\frac{1}{2\pi}\int_{-\infty}^{\infty}dte^{i\omega t}F_{11}(q,t)$$

$$=\frac{1}{\pi}\int_0^T dt\cos(\omega t)F_{11}(q,t) \tag{3}$$

with a similar expression for $S_{12}(q,\omega)$; T is the time interval over which the integrand has been computed.

Since our data are collected in a finite time interval $[0,T]$, one can expand the density fluctuations in Fourier series and create an alternative procedure to obtain the dynamic structure factors.[15] The result is

$$S_{11}(q,\omega)=\frac{1}{2\pi T}|\tilde{\rho}_1(\vec{q},\omega)|^2, \tag{4}$$

where $\tilde{\rho}_1(\vec{q},\omega)=\int_0^T dte^{i\omega t}\rho_1(\vec{q},t)$. This result can be generalized to give

$$S_{12}(q,\omega)=\frac{1}{2\pi T}\mathrm{Re}[\tilde{\rho}_1(\vec{q},\omega)\tilde{\rho}_2^*(\vec{q},\omega)]. \tag{5}$$

Although the calculation of the quantities of interest is reasonably well documented, we provide some of the details here to illustrate the bilayer contributions. Periodic boundary conditions restrict the wave vector $\vec{q}$ to the discrete values given by $\vec{q}=(q_x,q_y)=(2\pi/L)(n_x,n_y)$, where n_x, n_y are 0 (not both) or positive integers. We start by evaluating

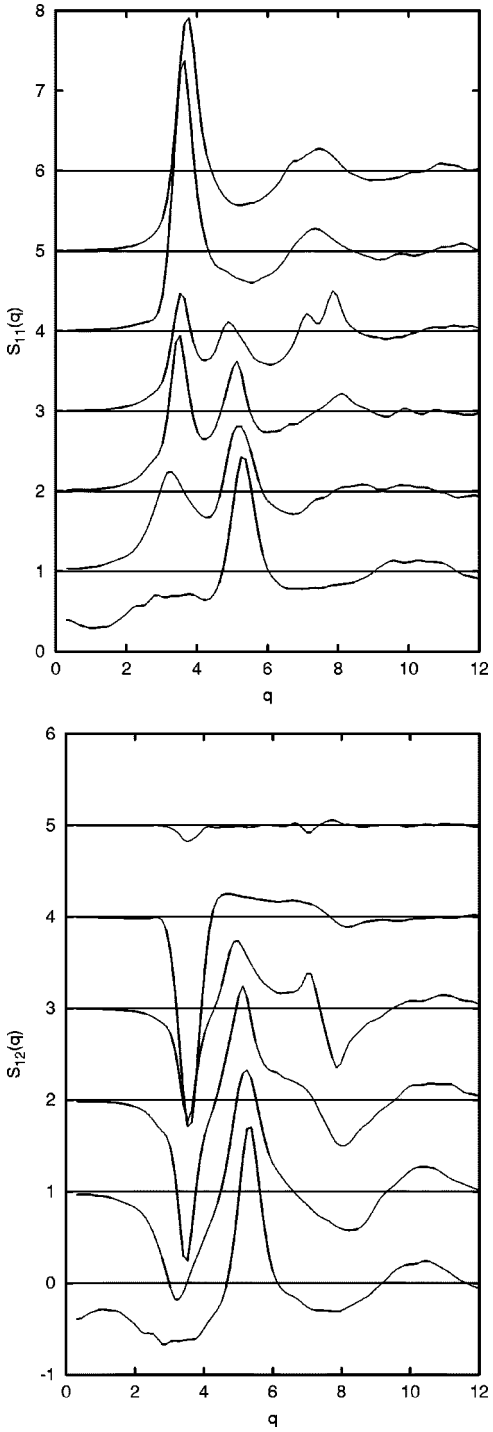

FIG. 1. (a) Intralayer static structure factor $S_{11}(q)$ for $\Gamma=80$ and $d=0.15$, 0.4, 0.6, 0.8, 1.1, and 2.0 from bottom to top. The plots are stacked for clarity. Quantities plotted in these figures are all in dimensionless units as defined in the text. Also note that smooth curves through our data points are used. (b) Interlayer static structure factor $S_{12}(q)$ for $\Gamma=80$ and $d=0.15$, 0.4, 0.6, 0.8, 1.1, and 2.0 from bottom to top. The plots are stacked for clarity.

$$C_1(q,t_j)=\sum_{k=1}^{N}\cos\{q_x x_k(t_j)+q_y y_k(t_j)\},$$

$$S_1(q,t_j)=\sum_{k=1}^{N}\sin\{q_x x_k(t_j)+q_y y_k(t_j)\},$$

$$C_2(q,t_j)=\sum_{k=N+1}^{2N}\cos\{q_x x_k(t_j)+q_y y_k(t_j)\},$$

$$S_2(q,t_j)=\sum_{k=N+1}^{2N}\cos\{q_x x_k(t_j)+q_y y_k(t_j)\}. \quad (6)$$

Since the system is isotropic, the correlation functions should depend only on the magnitude of the wave vector, and hence one averages over all possible $[n_x, n_y]$ values that give the same $q=|\vec{q}|$ to evaluate the expressions in Eq. (6). To enhance the statistics, we relax this condition slightly to include all possible $[n_x, n_y]$ values that give $\vec{q}$ vectors with approximately the same (to within 0.5%) magnitude. The intralayer and interlayer intermediate scattering functions are evaluated using

$$F_{11}(q,t_i)=\frac{1}{N(M-i)}\sum_{j=1}^{M-i}[C_1(q,t_j)C_1(q,t_j+t_i)+S_1(q,t_j)S_1(q,t_j+t_i)],$$

$$F_{12}(q,t_i)=\frac{1}{N(M-i)}\sum_{j=1}^{M-i}[C_2(q,t_j)C_1(q,t_j+t_i)+S_2(q,t_j)S_1(q,t_j+t_i)]. \quad (7)$$

Because of symmetry, either layer can be used to obtain F_{11}, and the roles of the two layers can be interchanged in the F_{12} expression. The smallest value of q (in units of $1/a$) compatible with our simulation is $2\pi/L=0.157$; others considered are $q=(2\pi/L)\sqrt{n_x^2+n_y^2}$. The dynamic structure factors $S_{11}(q,\omega)$ and $S_{12}(q,\omega)$ are then obtained using Eq. (3).

We have also used Eqs. (4) and (5) to evaluate $S_{11}(q,\omega)$ and $S_{12}(q,\omega)$ directly from the MD data. If $[0, T]$ is the time interval of the MD data and $\omega_n=2\pi n/T$, the appropriate formulas are

$$S_{11}(q,\omega_n)=\frac{1}{2\pi TN}\{[CC_1(q,\omega_n)+SS_1(q,\omega_n)]^2+[CS_1(q,\omega_n)-SC_1(q,\omega_n)]^2\},$$

$$S_{12}(q,\omega_n)=\frac{1}{2\pi TN}\{[CC_1(q,\omega_n)+SS_1(q,\omega_n)]\times[CC_2(q,\omega_n)+SS_2(q,\omega_n)]+[CS_1(q,\omega_n)-SC_1(q,\omega_n)]\times[CS_2(q,\omega_n)-SC_2(q,\omega_n)]\}, \quad (8)$$

where

$$CC_1(q,\omega_n)=\int_0^T dt\cos(\omega_n t)C_1(q,t),$$

$$CS_1(q,\omega_n)=\int_0^T dt\cos(\omega_n t)S_1(q,t),$$

$$SC_1(q,\omega_n)=\int_0^T dt\sin(\omega_n t)C_1(q,t),$$

$$SS_1(q,\omega_n)=\int_0^T dt\sin(\omega_n t)S_1(q,t), \quad (9)$$

and CC_2, CS_2, SC_2, SS_2 are obtained by replacing C_1 by C_2 and S_1 by S_2 in Eq. (9).

In order to reduce the noise caused by the finite trajectories, we multiply the intermediate scattering functions $F_{11}(q,t)$ and $F_{12}(q,t)$ by the Blackman filtering function,[16] which has been widely used in MD calculations. This procedure retains the original values for small and intermediate times and suppresses the possibly spurious values for large times. Although it may change the peak heights of the dynamic structure factors, it does not change the peak positions, nor does it seem to affect the frequency sum rules.

We have performed the following reliability checks on our calculations.

(i) Comparison with published $S(q,\omega)$ results for a single layer 2DEG;[15] for large interlayer separation ($d\sim 5$), a bilayer system is essentially equivalent to two uncorrelated single layers.

(ii) Comparison of $F_{11}(q,t)$ and $F_{12}(q,t)$ obtained directly using Eq. (7), and by Fourier transforms of $S_{11}(q,\omega)$ and $S_{12}(q,\omega)$ as obtained from Eq. (8).

(iii) Comparison of $S_{11}(q,\omega)$ and $S_{12}(q,\omega)$ obtained directly using Eq. (8) and by Fourier transforms of $F_{11}(q,t)$ and $F_{12}(q,t)$ as obtained from Eq. (7).

(iv) Comparison of structure factors $S_{11}(q)$ and $S_{12}(q)$ from $F_{11}(q,0)$ and $F_{12}(q,0)$, and those obtained as Hankel transforms of the pair distribution functions $g_{11}(r)$ and $g_{12}(r)$ which were obtained from our MD results.

(v) Confirmation of the frequency second moment sum rules for which exact expressions are well known.

III. RESULTS

We have generated MD data for selected values of Γ (80 and 40 in particular), and several values of d for each. These were used to obtain the dynamical correlation functions for several values of wave vector q as described in Sec. II. In this paper we restrict our detailed analysis and discussion to just one value of Γ: our previous studies[4,6] have shown that a bilayer with $\Gamma=80$ undergoes dramatic changes in its structure, pair correlation functions, diffusion coefficient, and single particle properties depending on the interlayer separation. Thus, we focus here on $\Gamma=80$ in our investigation of the collective properties of bilayers.

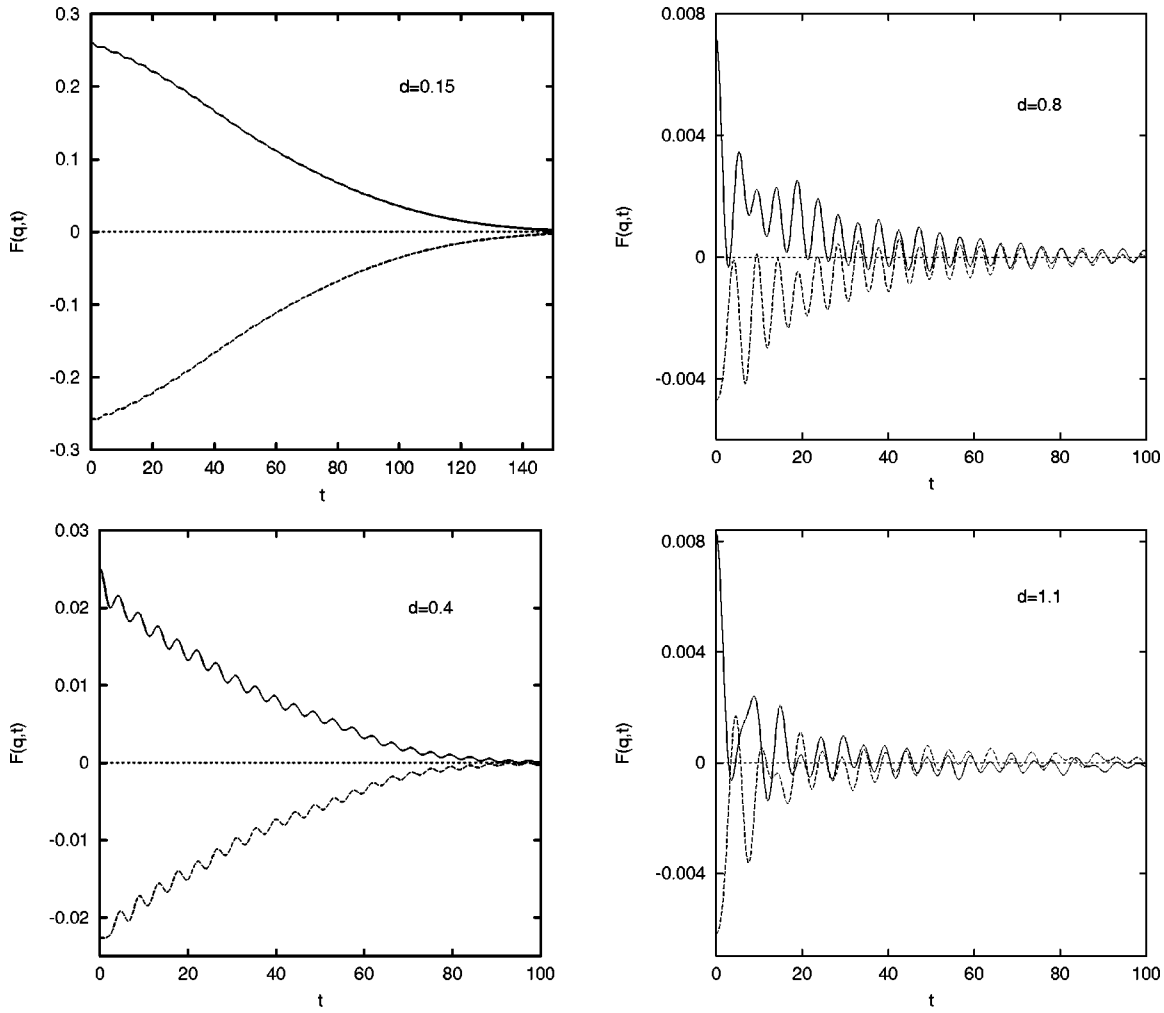

FIG. 2. Intermediate scattering functions $F_{11}(q,t)$ (solid) and $F_{12}(q,t)$ (dash) for $\Gamma=80$, $q=0.63$: (a) $d=0.15$, (b) $d=0.4$, (c) $d=0.8$, (d) $d=1.1$.

A. Static structure factor

Theoretical models often require the static structure factor as an input and their predictions of dynamical correlation functions are quite sensitive to its values. For a bilayer system, one needs both the intralayer $S_{11}(q)$ and the interlayer $S_{12}(q)$ static structure factors; reliable results are essential to produce theoretical predictions. These are normally obtained from transforms of the pair correlation functions according to

$$S_{11}(q)=F_{11}(q,0)=\int_{-\infty}^{\infty}S_{11}(q,\omega)d\omega$$

$$=1+2\pi n\int_0^{\infty}[g_{11}(r)-1]rJ_0(qr)dr,$$

$$S_{12}(q)=F_{12}(q,0)=\int_{-\infty}^{\infty}S_{12}(q,\omega)d\omega$$

$$=2\pi n\int_0^{\infty}[g_{12}(r)-1]rJ_0(qr)dr, \qquad (10)$$

where J_0 is the Bessel function of order 0.

However, this procedure requires that the oscillations of $g(r)$ about 1 for large r have died out. In MD calculations, $g(r)$ can be obtained for r less than half-the-box length only. For strongly coupled bilayers, oscillations persist in both $g_{11}(r)$ and $g_{12}(r)$ well beyond this distance, making evaluation of the structure factors using Eq. (10) inaccurate. Since $S(q)$ is exactly equal to the intermediate scattering function $F(q,t=0)$, this provides an alternative. It can also be obtained from the frequency integral of $S(q,\omega)$; however, MD requires that the values of q be discrete, starting with a well defined minimum value.

In Figs. 1(a) and 1(b) we have plotted the structure factors $S_{11}(q)$ and $S_{12}(q)$ for $\Gamma=80$, obtained as $F_{11}(q,0)$ and $F_{12}(q,0)$; the values of d are 0.15, 0.4, 0.6, 0.8, 1.1, and 2.0 as viewed from bottom to top. Note that q is in units of $1/a$ and d is in units of a. The graphs are stacked for clarity. We have also computed the structure factors using expressions (10); the agreement has been good for those values of d for which the transforms of g_{11} and g_{12} can be evaluated accurately for large r. As a further check, we also evaluated

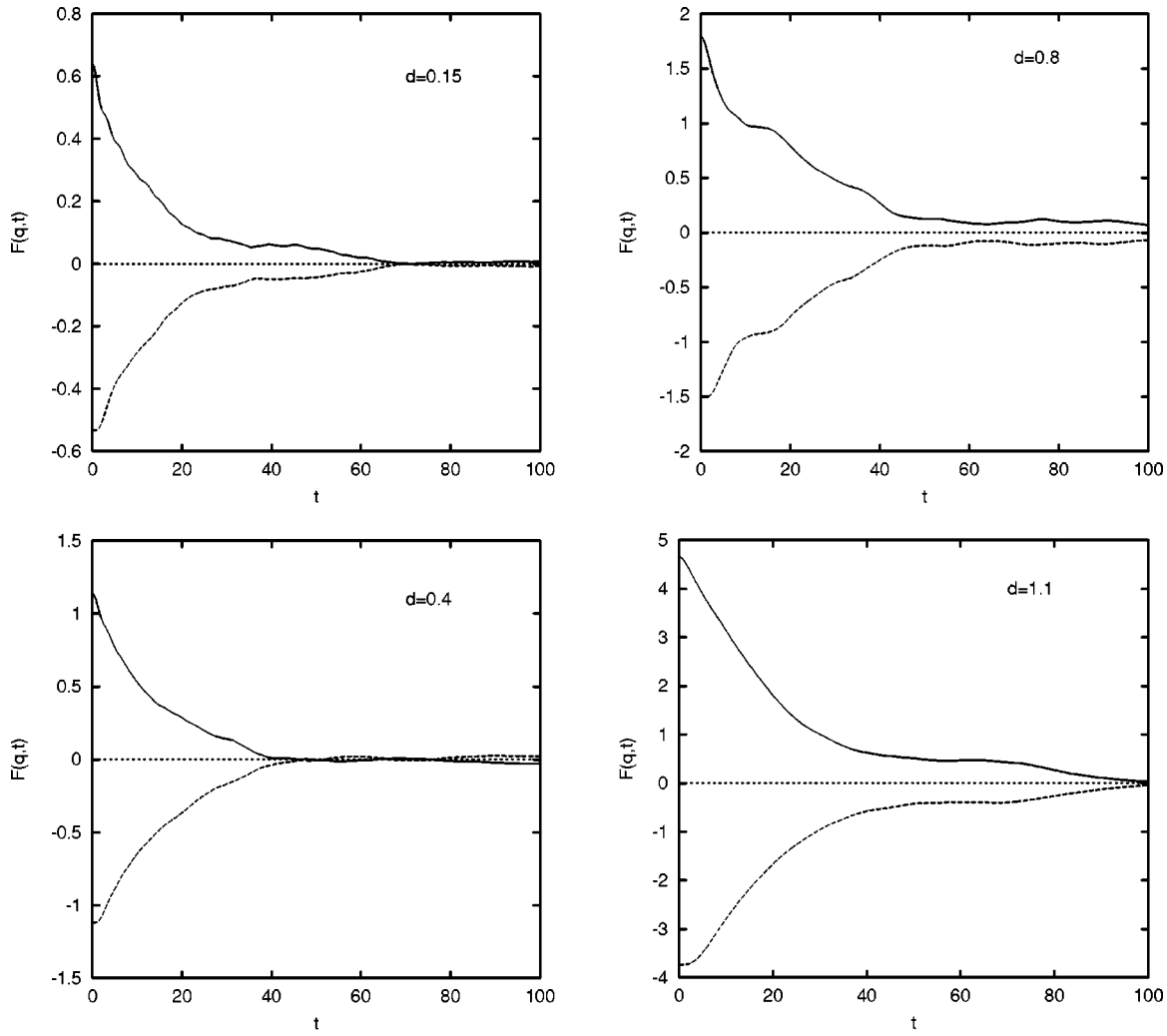

FIG. 3. $F_{11}(q,t)$ (solid) and $F_{12}(q,t)$ (dash) for $\Gamma=80$, $q=3.6$: (a) $d=0.15$, (b) $d=0.4$, (c) $d=0.8$, (d) $d=1.1$.

$$g_{11}(r)=1+\frac{1}{2\pi n}\int_0^\infty [S_{11}(q)-1]qJ_0(qr)dq,$$

$$g_{12}(r)=\frac{1}{2\pi n}\int_0^\infty [S_{12}(q)-1]qJ_0(qr)dq \qquad (11)$$

and compared these with their directly generated MD values; again the agreement is good.

For $d=1.1$ and 2.0, the behavior of $S_{11}(q)$ is typical of a single-layer 2DEG, in agreement with our previous findings[4,6] that a bilayer behaves very similar to a single-layer 2DEG for $d>1.5$. At $d=0$ it also behaves similar to a single layer with $\Gamma=80\sqrt{2}$. At both extremes, $S_{11}(q)$ displays just one dominant peak, its position being consistent with a hexagonal structure. For intermediate d we see the appearance of a second peak, and note that, while the heights of the two peaks change considerably, their positions change only marginally. In particular, $S_{11}(q)$ displays a considerable amount of structural details for $d=0.8$.

These structure functions must satisfy the perfect screening sum rule $S_{11}(q=0)=-S_{12}(q=0)$, which has the value 0.5 for $d=0$;[17] it decreases rapidly to 0 with increasing Γ and/or increasing d. For $d=0.15$ and our smallest q, this number is ≈ 0.3; for larger d it decreases rapidly.

For $\Gamma=80$ the interlayer function $S_{12}(q)$ undergoes a dramatic change as d increases. For small and large values of d its behavior is known: it approaches $S_{11}(q)-1$ as d approaches 0, and it becomes essentially zero for large values of d. For intermediate values of d we note certain distinctive features of $S_{12}(q)$. For $d=1.1$, $S_{11}(q)$ has almost reached its asymptotic large d behavior, but $S_{12}(q)$ has not. This implies that there is a strong interlayer correlation at $d=1.1$, but this has little effect on the correlations acting within a layer. For intermediate values of d (0.6 and 0.8), $S_{12}(q)$ displays a rather complex behavior: as the layers are brought closer together $S_{12}(q)$ is strongly affected while $S_{11}(q)$ is much less sensitive.

B. Dynamic structure factor

The intermediate scattering functions $F_{11}(q,t)$ and $F_{12}(q,t)$ were computed using Eq. (7) with a further averaging over a number of $\vec{q}$ vectors that yield a magnitude be-

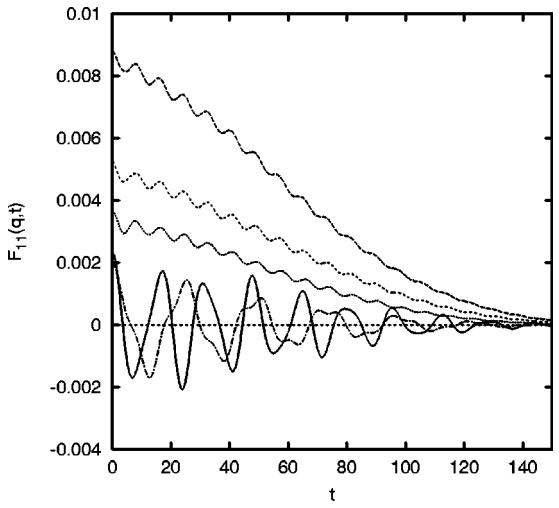

FIG. 4. $F_{11}(q,t)$ for $\Gamma=80$, $q=0.16$: $d=0.4$ (top), 0.6, 0.8, 2.0, and 5.0 (solid).

tween $1.005q$ and $0.995q$. We have evaluated these functions for q (in units of $1/a$) from $q_{\min}$ ($=0.16$) to 60 $q_{\min}$ ($=9.4$), and for d (in units of a) from 0.1 to 5, but we present only a representative sample of our results here. It should be noted that the values of $F_{11}(q,0)$ and $F_{12}(q,0)$ correspond exactly to $S_{11}(q)$ and $S_{12}(q)$.

Figure 2 shows $F_{11}(q,t)$ and $F_{12}(q,t)$ as functions of t (in units of τ) for $q=0.63$ and $d=$ (a) 0.15, (b) 0.4, (c) 0.8, and (d) 1.1. Two features are readily seen: there is an oscillatory behavior that becomes more pronounced as d increases, and it appears that $F_{12}(q,t)$ is almost a mirror image of $F_{11}(q,t)$. For large d (~ 5), where the system behaves as a single-layer 2DEG, $F_{12}(q,t)$ is very small, and $F_{11}(q,t)$ displays a strong oscillatory behavior about 0 for a long time with very little damping; this is in agreement with published MD results.[18] We see here that as d decreases, the damping increases and the oscillation height decreases and deviates from 0. The image phenomenon is indicative of the particles

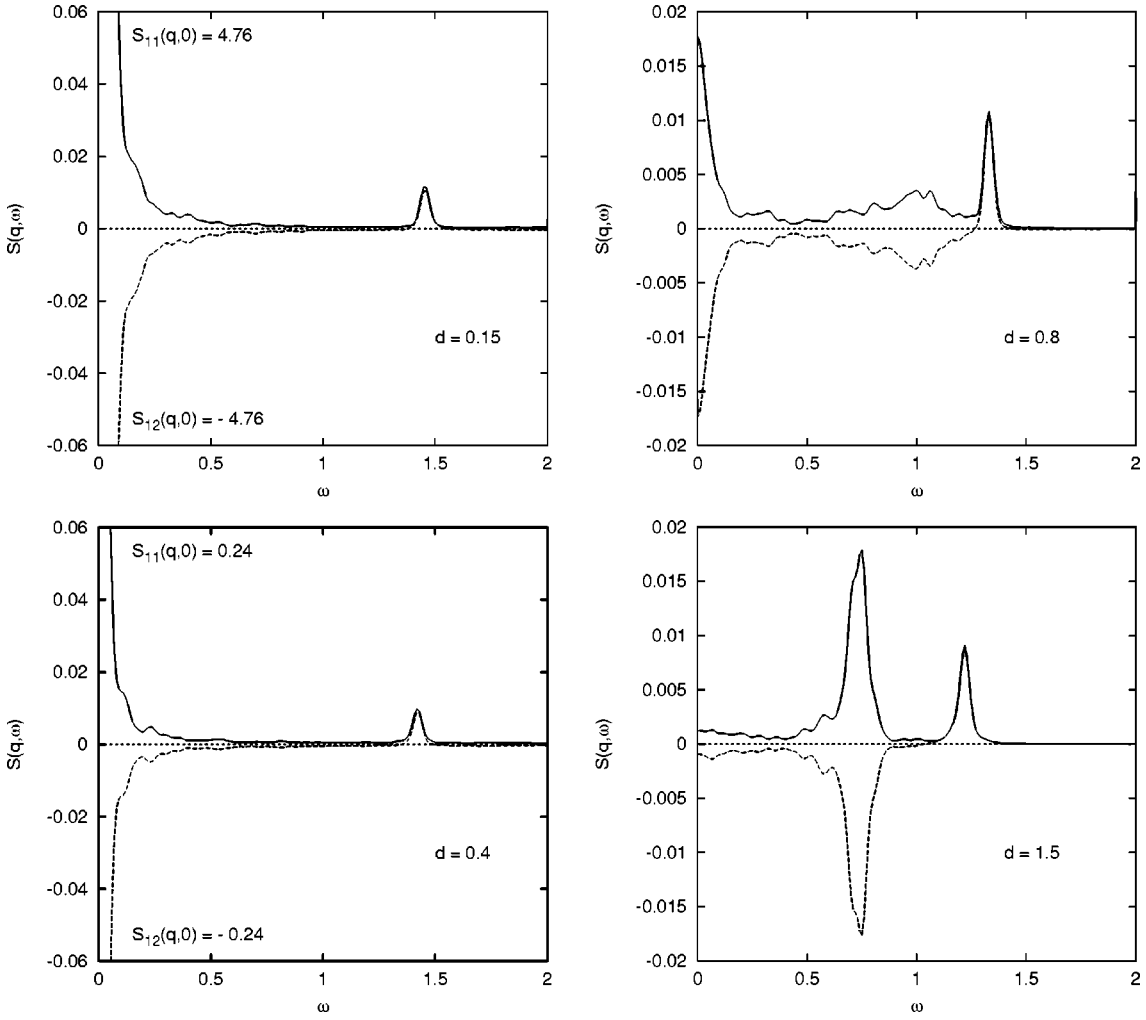

FIG. 5. Dynamic structure factors $S_{11}(q,\omega)$ (solid) and $S_{12}(q,\omega)$ (dash) for $\Gamma=80$, $q=0.63$: (a) $d=0.15$, (b) $d=0.4$, (c) $d=0.8$, (d) $d=1.5$.

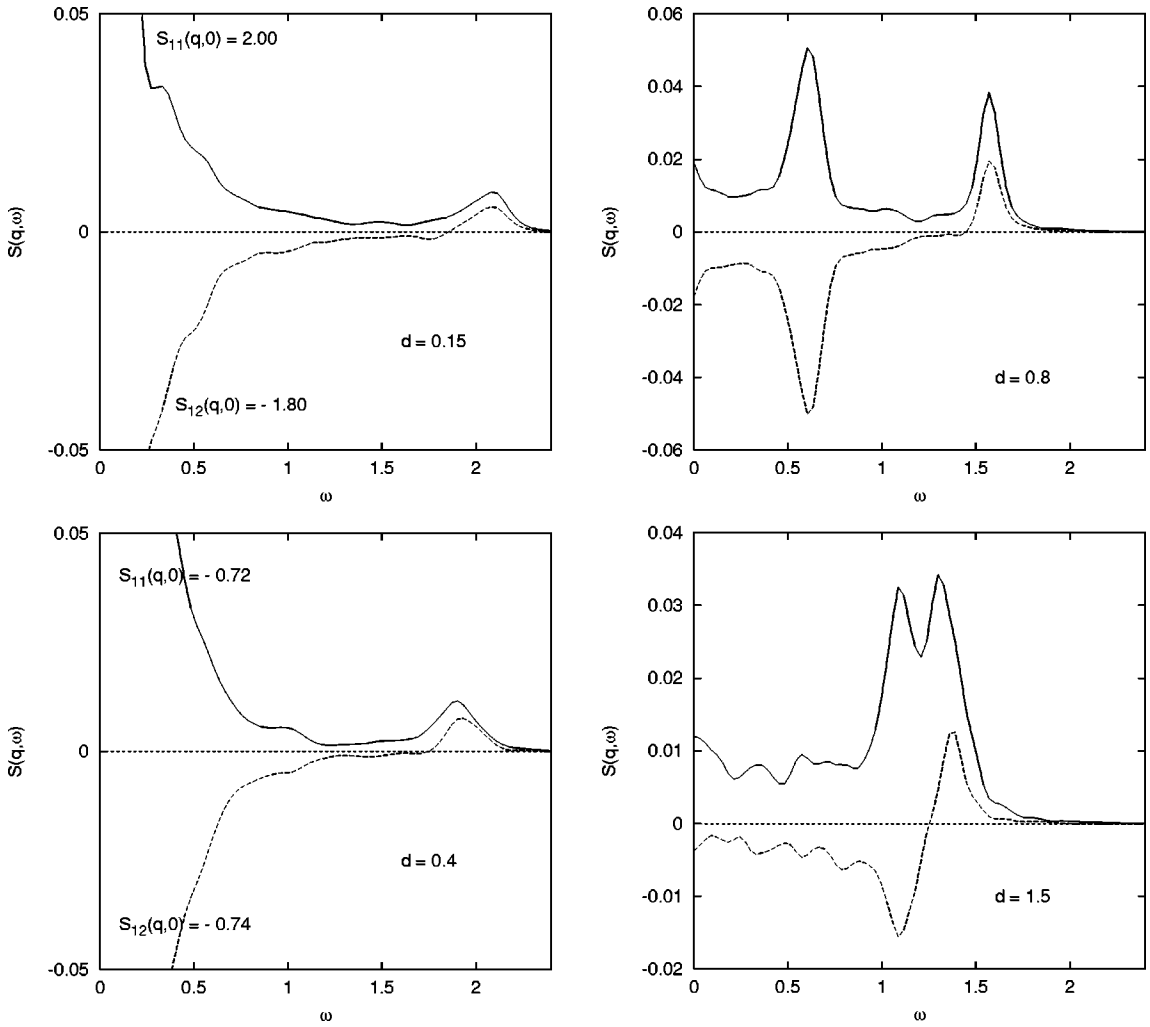

FIG. 6. $S_{11}(q,\omega)$ (solid) and $S_{12}(q,\omega)$ (dash) for $\Gamma=80$, $q=1.9$: (a) $d=0.15$, (b) $d=0.4$, (c) $d=0.8$, (d) $d=1.5$.

in the two layers oscillating in phase and 180° out of phase. Figure 3 shows similar plots for a value of $q=3.6$, near the main peak of $S_{11}(q)$ of a single-layer 2DEG; the functions decay faster and the oscillations have also almost died out. For larger values of q, the decay is almost monotonic and fast, and the functions are closer to their respective ideal gas values. Figure 4 shows a plot of $F_{11}(q,t)$ only for $q=0.157$ (our smallest) and $d=0.4$, 0.6, 0.8, 2, and 5. This illustrates the significant effect of d on the intermediate scattering function $F_{11}(q,t)$. As noted before, $F_{12}(q,t)$ will be nearly a mirror image of $F_{11}(q,t)$.

The Fourier transforms $S_{11}(q,\omega)$ and $S_{12}(q,\omega)$ of the intermediate scattering functions are of special importance because they may be determined experimentally, and because peaks in these functions occurring at $\omega\neq 0$ are related to the collective properties of the system. In Fig. 5 plots of these functions are displayed for small q $(=0.63)$ and $d=$(a) 0.15, (b) 0.4, (c) 0.8, (d) 1.5; note that ω is in units of $1/\tau$. For such values of q, one expects collective behavior. For the two smallest values of d, there is one clear peak in $S_{11}(q,\omega)$ and a coincident positive peak in $S_{12}(q,\omega)$, in addition to the dominant central peak. Other features are (i) $S_{12}(q,\omega)$ is almost a mirror image of $S_{11}(q,\omega)$ except at the positive side peak where they merge almost completely, (ii) the positions of the side peak are identical for both $S_{11}(q,\omega)$ and $S_{12}(q,\omega)$, (iii) the smaller the value of d, the stronger is the central component, which for $d=0.15$, completely dwarfs the collective peak, and (iv) the height of the noncentral peak changes only slightly as d changes. The strong central peak coupled with one collective side peak structure is typical of many systems, but our bilayer system evolves into a two side peak structure at the expense of the central peak as the interlayer separation is further increased. For example, at $d=0.8$ [Fig. 5(c)] another side peak is starting to form in $S_{11}(q,\omega)$ along with its mirror image in $S_{12}(q,\omega)$ and the central peak, though still present, has become considerably smaller. As d increases, this second peak becomes stronger and the central peak almost nonexistent as shown in Fig. 5(d). This structure disappears only when $S_{12}(q,\omega)$ becomes negligible, which in our case does not quite happen even for $d=5$.

The two side peak structure persists as q increases; this is seen in Fig. 6 where $S_{11}(q,\omega)$ and $S_{12}(q,\omega)$ are displayed for $q=1.9$ and $d=$ (a) 0.15, (b) 0.4, (c) 0.8, (d) 1.5. Plots for the two smaller values of d are quite similar to their counterparts in Fig. 5, except that the side peaks have moved to

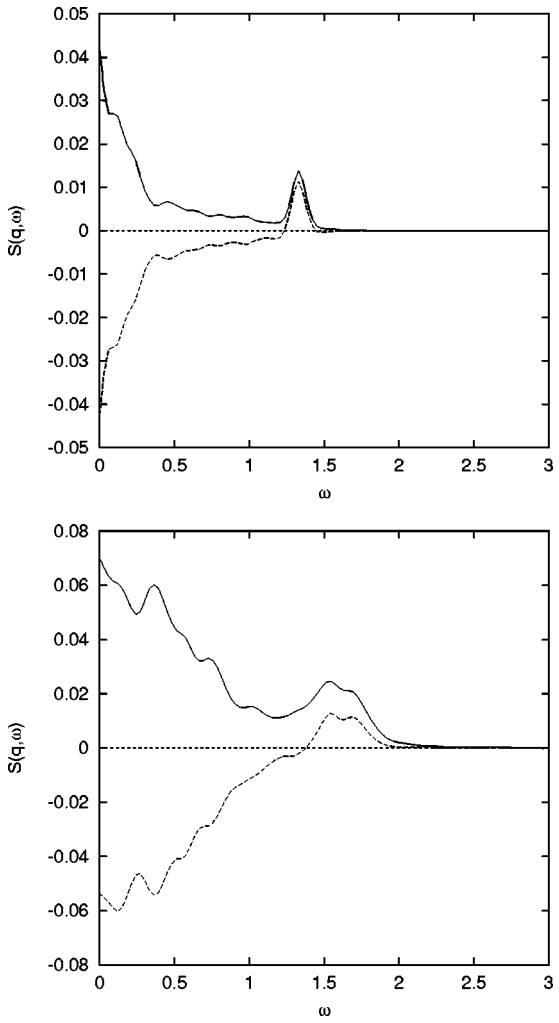

FIG. 7. $S_{11}(q,\omega)$ (solid) and $S_{12}(q,\omega)$ (dash) for $\Gamma=40$, $d=0.8$: (a) $q=0.63$, (b) $q=1.9$.

the right in frequency. For $d=0.8$, the two peaks are now farther apart when compared to Fig. 5(c), while for $d=1.5$, they have almost merged. In addition, heights of this second peak of $S_{11}(q,\omega)$ and $S_{12}(q,\omega)$, which were essentially the same for $q=0.63$, are now very different. The two side peak structure was observed even for $d=5$, $q=0.63$, but reduced to a single side peak beyond $d=1.5$ for $q=1.9$. For higher values of q ($\geqslant 3$), close to and beyond the main peak of $S_{11}(q)$, and for all values of d, $S_{11}(q,\omega)$ and $S_{12}(q,\omega)$ essentially go over to their respective ideal gas values.

As a review of our findings, taking an example of $d=0.8$, $S_{11}(q,\omega)$ displays just a single side peak for $q=0.16$ (smallest q accessible by our MD system). The second side peak starts to manifest itself around $q=0.6$ and grows in intensity at the expense of the first peak as q increases. The double peak disappears around $q=2.5$, and finally the remaining single peak disappears around $q=4$ where $S_{11}(q,\omega)$ behaves similar to an ideal gas. Such a behavior is seen for $\Gamma=80$ if $d>0.6$.

To see if the double side peak structure appears for smaller values of Γ, we have plotted $S_{11}(q,\omega)$ and $S_{12}(q,\omega)$ for $\Gamma=40$ and $d=0.8$ for (a) $q=0.63$, (b) $q=1.9$ in Fig. 7. A comparison with the corresponding Figs. 5(c) and 6(c) clearly shows the absence of such a feature. However the double peak structure is seen for large d (>1.5) and small q (<1), similar to the ones observed for $\Gamma=80$. Our findings are completely consistent with recent MD calculations reported for $\Gamma=40$.[19]

Our results indicate that a double side peak structure in $S_{11}(q,\omega)$ and $S_{12}(q,\omega)$ is quite a common feature in bilayer systems. Based on our extensive analysis, we conclude that this structure is present for $d>1.5$ and small q (<2), for all Γ. How far this structure extends in d depends on Γ: for $\Gamma=40$ the minimum value of d is around 1.5, while for $\Gamma=80$ it is around 0.6. The interesting question is what this structure implies concerning the plasmon modes of the system. Our studies show that the two side peaks in $S_{11}(q,\omega)$ and $S_{12}(q,\omega)$ and their respective positions and heights play a significant role in the propagation and dispersion of the plasmon modes, especially the out-of-phase mode. Several theoretical models have predicted the existence of two collective longitudinal modes in a bilayer system; these are best analyzed not through $S_{11}(q,\omega)$ and $S_{12}(q,\omega)$ directly, but through two correlation functions which are linear combinations of them. This is a subject of a subsequent paper that deals in detail with collective modes of a bilayer system and their dispersion relations.[20]

IV. CONCLUSIONS

We have performed extensive MD calculations for strongly coupled, classical symmetric electronic bilayers. The focus of this paper has been on static and dynamic structure factors, and these have been analyzed for many selected values of the interlayer separation d and wave vector q. A relatively high value of Γ ($=80$) was chosen for the study as such a system, while displaying the characteristics of a liquid at small and large values of d, exhibits some features of a solid for intermediate values of d. A thorough analysis of their behavior as a function the wave vector and interlayer separation has revealed new and distinctive features present in bilayer systems. It is seen that the dynamic structure factors possess a double side peak structure for intermediate values of q and d, a feature that is not seen for smaller values of Γ.

Although some attempts have been made to develop theoretical models of a bilayer electronic system, their predictions could not be checked because of the unavailability of MD results. In addition, theoretical models often require static structure factors as inputs. Experimental results, few as they may be, involve real systems with quantum effects and complex interaction potentials and hence are not immediately amenable for comparison with theory. Here, and in previous papers, we have provided some of the much-needed MD results for static and dynamic correlation functions: these should offer an immediate test of any theoretical model.

ACKNOWLEDGMENTS

This research was supported in part by a grant from the Academic Research Program (ARP) of the Department of National Defence, Canada.

[1] G. Goldoni and F. M. Peeters, Phys. Rev. B **53**, 4591 (1996).
[2] J.-J. Weis, D. Levesque, and S. Jorge, Phys. Rev. B **63**, 045308 (2001).
[3] Z. Donkó and G. J. Kalman, Phys. Rev. E **63**, 061504 (2001).
[4] S. Ranganathan, R. E. Johnson, and K. N. Pathak, Phys. Rev. E **65**, 051203 (2002).
[5] I. V. Schweigert, V. A. Schweigert, and F. M. Peeters, Phys. Rev. Lett. **82**, 5293 (1999).
[6] S. Ranganathan and R. E. Johnson, Phys. Rev. E **67**, 041201 (2003).
[7] L. Swierkowski, D. Neilson, and J. Szymanski, Aust. J. Phys. **46**, 423 (1992); L. Liu, L. Swierkowski, D. Neilson, and J. Szymanski, Phys. Rev. B **53**, 7923 (1996).
[8] R. K. Moudgil, P. K. Ahluwalia, and K. N. Pathak, Phys. Rev. B **56**, 14 776 (1997).
[9] G. J. Kalman, V. Valtchinov, and K. I. Golden, Phys. Rev. Lett. **82**, 3124 (1999).
[10] K. I. Golden and G. J. Kalman, Phys. Plasmas **7**, 14 (2000); K. I. Golden and G. Kalman, J. Phys. A **36**, 5865 (2003).
[11] T. B. Mitchell, J. J. Bollinger, D. H. E. Dubin, X.-P. Huang, W. M. Itono, and R. H. Baughmann, Science **282**, 1290 (1998).
[12] D. S. Kainth, D. Richards, A. S. Bhatti, H. P. Hughes, M. Y. Simmons, and D. A. Ritchie, Phys. Rev. B **59**, 2095 (1999).
[13] P. G. Bolcatto and C. R. Proetto, Phys. Rev. Lett. **85**, 1734 (2000).
[14] R. E. Johnson and S. Ranganathan, Phys. Rev. E **63**, 056703 (2001).
[15] H. Totsuji and H. Kakeya, Phys. Rev. A **22**, 1220 (1980).
[16] M. P. Allen and D. J. Tildesley, *Computer Simulation of Liquids* (Oxford Science, Oxford, 1990).
[17] V. I. Valtchinov, G. Kalman, and K. B. Blagoev, Phys. Rev. E **56**, 4351 (1997).
[18] S. W. De Leeuw, J. W. Perram, and E. R. Smith, Physica A **119**, 441 (1983).
[19] Z. Donkó, G. J. Kalman, P. Hartmann, K. I. Golden, and K. Katusi, Phys. Rev. Lett. **90**, 226804 (2003).
[20] S. Ranganathan and R. E. Johnson. Phys. Rev. B **69**, 085310 (2004), the following paper.